

Electronic and positronic studies of zinc-blend boron phosphide BP underpressure

M. Sehil^{1,*}, H. Abid¹, A. Lachebi¹, Y. Al-Douri²

¹⁾ Applied Materials Laboratory. University research centre University of Sidi-Bel-Abbès, 22000 Algeria.

²⁾ School of Microelectronic Engineering, University Malaysia Perlis, 02600 Jejawi Arau, Perlis, Malaysia.

Abstract

We analyze the effect of the pressure variations on the electron and the positron distributions in the boron phosphide. On the basis of the pseudopotential band structure calculations (EPM) and the independent particle approximation (IPM), the electron and the positron wave functions are derived, respectively. The resulting wave functions are used to compute the corresponding charge densities along the $\langle 111 \rangle$ axis. The integrated electron-positron momentum densities, for different pressures, are calculated along the (001) and (110) directions. The results are used to analyze the evolution of the bonding properties and to predict how pressure could affect positron annihilation results in the boron phosphide.

Keywords: Positron annihilation, Empirical pseudo-potential, Independent Particle Model, Charge densities, Momentum densities and Anisotropy.

1. Introduction

There is a considerable interest in solids formed from atoms with low atomic numbers because of the potential unique properties of these materials [1]. The relatively strong chemical bonding characteristic of the second-row atoms are associated with these properties. This leads to large elastic constants which, in turn, are related to hardness and good thermal conductivities.

Boron compounds constitute a family of compounds that are written as BX, X being Phosphor P, Nitrogen N or As, which are group-V elements. Generally, compounds belonging to a given family have similar properties that gradually change with increasing atomic number. As the best example, one may consider III-V compounds. These semiconductors have the same zinc-blend crystalline structure with tetrahedral environment and the same kind of semiconducting electronic structure. Boron Phosphide BP with zinc-blend structure [the space grouping for the zinc-blend structure is $F\bar{4}3m(T_d^2)$] has found of a great interest during the past few years because it shows promising electrical, mechanical and thermal properties [2]. Boron Phosphide is very unstable under humid conditions make growing of single crystals extremely difficult. The single crystal growth of boron phosphide

*) For correspondence, E-mail: m_sehil@yahoo.fr.

(BP) is obtained by employing the high pressure flux method and chemical vapor deposition (CVD) process [2]. According to the Phillips scale of ionicity, BP is one of the most covalent of the III-V semiconductors and is known to have one of the smallest heteropolar gaps of the III-V compounds semiconductors [3]. Like diamond and BN, the compound BP is known to be a hard material and the only report of its bulk modulus is an interpolation based on empirical relations for the elastic constants. The bulk modulus of BP was measured to be 172 GPa [4]. A.Lichanot et al [5] take the bulk modulus B_0 to be 166 GPa and W.Lambrecht et al [6] take the bulk modulus B_0 to be 172 GPa and the first derivative of bulk modulus B'_0 to be 3.7. However R. Orlando et al [7] take B_0 to be 170 GPa. In other work, one takes the bulk modulus B_0 to be 152 GPa and the first derivative of bulk modulus to be 4.3 [8]. In our calculations, we take the bulk modulus B_0 to be 172 GPa and the first derivative of bulk modulus to be 3.76 [9].

Boron phosphide is expected to undergo a structural phase transformation from its zinc-blend phase to a rocksalt phase at a pressure up to 160 GPa, according to total energy pseudopotential calculations within the local density approximation [10]. It is of theoretical interest to investigate the high-pressure behavior of boron phosphide, nevertheless, the major experimental difficulties in doing X-ray diffraction studies of BP under extreme pressure are due to its low atomic number. This results in the diffraction intensities decreasing rapidly when reaching extreme pressure the sample becomes very thin [8].

In the present work, we determine the best set of form factors required in computing the boron phosphide properties using an adjusted local pseudopotential method.

Because Boron Phosphide is isoelectronic to SiC [11], it is convenient to think of BP as derived from SiC by a replacement of the silicon atoms by phosphorous and the carbon atoms by those of boron. Then, in order to study the behaviour of the electronic states of BP, at the Γ , X and L points in the Brillouin zone for different compressed volumes, one can determined empirically the pressure derivatives of the pseudopotential form factors of BP by fitting the calculated structure to those of SiC [12]. In our calculations, we take the linear and sublinear pressure derivatives of the pseudopotential form factors of BP obtained by B.Bouhafs et al [9].

The study of positron interactions with electrons in condensed matter and the development of positrons as a probe of electronic structure have a long documented history [13]. From the early stage of this history, the angular correlation of annihilation radiation (ACAR) in semiconductors has been one of the interesting targets. Puska [14] has modelled the positron states in elemental and compound semiconductors with an atomistic theory incorporating many-particle screening effects. In some materials, such as semiconductors, positron annihilation momentum density measurements are made to obtain some information about the electronic structure of solids [15, 16].

As a result of its positive charge the crystal potential experienced by a positron differs from that experienced by an electron since the positron is strongly repelled from the regions of the ion cores and hence annihilates preferentially with the valence electrons. There are no positron-positron interactions since it is assumed that there is at most one positron in the crystal at any time. An additional potential term comes from the positron-electron correlation.

There has been some attempt to study the positron wave function in compound semiconductors so far few calculations have been reported on their ACAR lineshapes at normal and high pressures. This has prompted us to take such a calculation in boron phosphide.

The other aspect of this work is that a useful test of the theories of positron annihilation in semiconductors is the pressure dependence of the annihilation rate in

compound semiconductors. The study of electronic properties of semiconductors using the electronic and positronic charge densities occupies an important place. Most of the work thus far has concerned electron charge densities where it has been found useful for the understanding of the chemical bonds and the modifications of band structures by interstitial impurities [17]. Positron charge densities provide complementary informations.

The Gaussian pseudo-potential method is used for the calculation of the electron wave functions and we suggest an approach that permits the calculation of positron wave function in the independent particle approximation (IPM). The ionic potential may be expressed in terms of the point charge situated at the lattice sites. Computational details are given in section 3 and section 4 is devoted to the discussion of the results.

2. Calculations

Our path of calculation to the electron-positron momentum density is essentially that followed in the work of Stroud [18], wherein the solutions to the single particle electron and positron schrödinger equations are represented as plane wave expansions involving lattice vectors. The calculation of valence electron wave functions was based on the empirical pseudopotential method (EPM) and has proven a powerful tool for understanding electronic energy band structure of semiconductors.

Let us define our empirical pseudopotential parameters (EPP) of a semiconductor as a superposition of the pseudo-atomic potential of the form:

$$V(\mathbf{r}) = V_L(\mathbf{r}) + V_{NL}(\mathbf{r}) \quad (1)$$

where V_L and V_{NL} are local and non local parts, respectively. In these calculations, we neglected the non local part. We regard the Fourier components of $V_L(\mathbf{r})$ as the EPP local parameters. We determine the EPP parameters by the nonlinear least squares method in which all the parameters are simultaneously optimized under a defined criterion of minimizing the root mean square (RMS) deviation.

Our nonlinear least squares method requires that the (RMS) deviation of the calculated level spacing's (LS) from the experimental ones defined by:

$$\delta \approx \left[\frac{\sum_{(i,j)} (\Delta E^{(i,j)})^2}{(m-n)} \right]^{\frac{1}{2}} \quad (2)$$

Should be minimum with:

$$\Delta E^{(i,j)} \approx E_{\text{exp}}^{(i,j)} - E_{\text{cal}}^{(i,j)} \quad (3)$$

where $E_{\text{exp}}^{(i,j)}$ and $E_{\text{cal}}^{(i,j)}$ are the observed and calculated LS's between the i th state, at the wave vector $\mathbf{K}=\mathbf{K}_i$ respectively, among the chosen pairs (i,j) and N is the number of the EPP parameters.

The calculated energies given by solving the EPP secular equation depend nonlinearly on the EPP parameters. The starting values of the parameters are improved step by step, by iterations until δ is minimized. We denoted the parameters by P_u ($u = 1, 2, 3 \dots N$) and write as $P_u(n+1) + \Delta P_u$, where $P_u(n)$ is the value at the n th iteration.

The corrections ΔP_u are determined simultaneously by solving a system of linear equation [19]:

$$\sum_{u=1} \left[\sum_{(i,j)} m.(q_u^i - q_u^j).(q_{u'}^i - q_{u'}^j) \right] = \sum_{(i,j)} m.[E_{\text{exp}}^{(i,j)} - E_{\text{cal}}^{(i,j)}(n)](q_{u'}^i - q_{u'}^j) \quad (4)$$

$$U' = 1, 2, 3 \dots N$$

where $E_{\text{cal}}^{(i,j)}(n)$ is the value at the n th iteration. The quantity Q_u is given by:

$$Q_u^j = \sum_{q,q'} [C_q^i(K_i)] \left[\frac{\delta H(K_i)}{\delta P_u} \right]_{qq'} C_{q'}^i(K_i) \quad (5)$$

$H(K_i)$ is the pseudo-hamiltonian matrix at $K = K_i$, in the plane wave representation (P.W), and the i th pseudo-wave function at $K = K_i$ is expanded as :

$$\Psi_{K_i}^i(r) = \sum_q C_q^i(K_i) \exp[i(K_i + K_q)r] \quad (6)$$

K_q being the reciprocal lattice vector. Equation (4) shows that all of the parameters are determined automatically in an interdependent way. The pseudo-wave functions $\Psi_{K_i}^i(r)$ are calculated at each iteration using all the PW's with K_q satisfying the following relation:

$$(\hbar^2/2m) \left| |K + K_q|^2 - |K|^2 \right| \leq E_{\text{max}} \quad (7)$$

A choice of $E_{\text{max}} = 14$ in units of $(\hbar^2/2m)$ ($2\pi/a$) turns out to be practical.

Good starting values of the EPP parameters were carefully chosen by test-working with the smaller to full sized Hamiltonian matrices ($E_{\text{max}} = 14$). Iteration convergence was exceedingly good. For example, only about ten iterations were enough to determine the EPP parameters. The valence electron density is defined as:

$$\rho(r) = 2e \sum_n \sum_K |\varphi_{nK}(r)|^2 \quad (8)$$

where $\varphi_{nK}(r)$ is the wave function of the valence electron with the wave vector k in the n th valence band and e is the electron charge. The summations are taken over the occupied states. This has the Fourier transform given by:

$$\rho(G) = \frac{1}{\Omega} \int \rho(r) \exp(iGr) d^3r \quad (9)$$

Assuming that there is one positron for many electrons, there is no exchange effect because there is no positron-positron interaction. The positron potential is purely coulombic in nature.

There is a repulsive ion core potential and an attractive Hartree potential. In addition to these two, there is a third effect which comes from the electron-positron correlation. Thus the total positron potential can be expressed as:

$$V_p(r) = V_i(r) + V_c(r) + V_{ep}(r) \quad (10)$$

Where $V_i(r)$, $V_c(r)$ and $V_{ep}(r)$ are the ionic, coulomb and electron-positron correlation potentials, respectively. The electron-positron potential is a slow function of the electron density. In the interstitial region, $V_{ep}(r)$ is flat and swamped by the potentials $V_i(r)$ and $V_c(r)$ in the ion core region. Hence, it is not considered here. $V_i(r)$ is expressed as:

$$V_i(r) = \sum_{\alpha} \sum_{R_j} \sum_{R_n} V_i^{\alpha}(r - R_n - R_j^{\alpha}) \quad (11)$$

Because $V_i(r)$ is a periodic and zinc-blend structure, R_n denotes the set of all Bravais lattice vectors and R_j^{α} is a non-primitive vector of a two-atoms basis.

If we choose the origin of coordinates half way between the two atoms of the unit cell, we have:

$$V_i(G) = V_s(G) \cdot \cos(G) + V_a(G) \cdot \sin(G) \quad (12)$$

where $V_s(G)$ and $V_a(G)$ are, respectively, the symmetric and the antisymmetric contributions of the atomic potentials and G is a reciprocal lattice vector.

In the point core approximation, $V_i^{\alpha}(r)$ is expressed as:

$$V_i^{\alpha}(r) = \frac{Z_{\alpha} e^2}{r} \quad (13)$$

Then, $V_s(G)$ and $V_a(G)$ are expressed as:

$$\begin{aligned} V_s(G) &= V_1(G) + V_2(G) \\ V_a(G) &= V_1(G) - V_2(G) \end{aligned} \quad (14)$$

where $V_1(G)$ and $V_2(G)$ are the contributions of the cation and the anion, respectively. The quantities $V_1(G)$ and $V_2(G)$ are given by:

$$V_1(G) = \frac{2N}{\Omega} \cdot \frac{4\pi Z_1 e^2}{|G|} \quad \text{and} \quad V_2(G) = \frac{2N}{\Omega} \cdot \frac{4\pi Z_2 e^2}{|G|} \quad (15)$$

(Z_1e) and (Z_2e) are the charges of the cation and the anion respectively and Ω is the unit cell volume. On the other hand, the electron-positron coulomb potential is expressed as:

$$V_c(r) = -e^2 \int \frac{\rho_e(r')}{|r-r'|} d^3r' \quad (16)$$

The positron wave function was represented by a plane wave as:

$$\psi_+(r) = \left(\frac{1}{\Omega}\right)^2 \sum_G A(G) \exp(iGr) \quad (17)$$

The coefficients A (G) are found out by solving the equation:

$$\sum \left[|G^2 - E| \delta_{G,G'} + V_+(|G - G'|) \right] A(G') = 0 \quad (18)$$

The resulting positron wave functions are used to compute the positron charge density:

$$\rho_p(r) = \left| \psi_{n=1,k=0}^+(r) \right|^2 \quad (19)$$

The positron, after entering the solid, gets thermalized and attracts the surrounding valence electrons forming an electron-positron pair. This pair subsequently gets annihilated to emit two gamma rays. The probability of annihilation of the electron-positron pair with momentum p is proportional to the pair momentum density:

$$\rho^{2\gamma}(p) = const. \sum_{nk} \eta_n(k) \left| \int \psi_{nk}(r) \cdot \psi_+(r) \cdot e^{-ipr} d^3r \right|^2 \quad (20)$$

where $\eta_n(k)$ is the occupation number.

3. Results

The table1 gives the parameters of boron phosphide used in this calculations together with other parameters of previous studies at $p=0$ GPa. The form factors V (G^2) are given in Rydberg. It is interesting to note from Table1 that the antisymmetric form factors of BP are all quite small, the largest being 0.034 Ryd, indicating that Boron Phosphide is essentially purely covalent at normal pressure. One can explain the covalent character by Boron potential properties.

a (0.1nm)	$V_s(3)$	$V_s(8)$	$V_s(11)$	$V_a(3)$	$V_a(4)$	$V_a(11)$
4.53 ^a	-0.3794 ^a	0.0870 ^a	0.0916 ^a	0.010 ^a	0.023 ^a	0.034 ^a
4.5383 ^b	-0.373 ^b	0.085 ^b	0.099 ^b	0.010 ^b	0.023 ^b	0.034 ^b
4.526 ^c	---	---	---	---	---	---
4.538 ^d	---	---	---	---	---	---

Table 1: Adjusted symmetric and antisymmetric form factors correspond with lattice parameter. ^a: Ref. [8] (these parameters are used in the present work), ^b: Ref. [20], ^c: Ref. [5], ^d: Ref. [21].

The very attractive B potential competes with the element V's potential for the valence charge creating a situation of small heteropolarity and consequently small ionicity. According to the Phillips and Van Vechten scale of ionicities, Boron Phosphide has one of the lowest ionicity in the III-V group ($f_i = 0.006$) [3]. The key energies of BP both with and without V_{NL} , at selected symmetry points in the Brillouin zone, are given in table 2 and the linear $\frac{dE_{nk}}{dp}$ and sub linear $\frac{d^2E_{nk}}{dp^2}$ pressure coefficients of BP, used to study the electronic state at high symmetry points Γ , X and L (with respect to the top of the valence bands) in the Brillouin zone, for different compressed volumes, are listed in table 3.

Then, the calculated energies at high symmetry points Γ , X and L are given with the following equation: $E_i(p) = E_i(0) + \alpha_i p + \beta_i p^2$, where α_i and β_i are, respectively, the linear and the quadratic pressure coefficient at each high symmetry point Γ , X and L. The energy band gaps and the hydrostatic pressures are given, respectively, in (eV) and in (GPa). The calculated fundamental energy gaps versus hydrostatic pressure are listed in the table 4.

As was illustrated in Table 4, we notice that the energy gap $E_{\Gamma\Gamma}$ increases with the pressure until the value of 90 GPa where the band gap decreases when the pressure increases. The situation is quite different for the $E_{\Gamma X}$ band gap because the latter decreases with the pressure until the value of 60 GPa and from this value the band gap $E_{\Gamma X}$ increases with pressure. For the case of the $E_{\Gamma L}$ band gap, there is a linear increase of this energy gap with the pressure.

The fundamental gap ($\Gamma_{15}^V \rightarrow X_1^C$) decreases from 2.180 to 2.0984 eV (3.74%) when the initial volume is compressed and reduced by 20%. For the same compressed volumes we observe, in contrast, an important rise of the energy gap by about 66.5% and 28.5% for Γ_C and L_C , respectively. One can state that the $E_{\Gamma\Gamma}$ band gap is more sensitive to the pressure variations than those of $E_{\Gamma X}$ and $E_{\Gamma L}$. We can deduce that the pressure affects qualitatively and quantitatively the band structure of the boron phosphide.

	V _L	V _{NL}
$\Gamma_{15}^V - \Gamma_1^C (eV)$	5.25 [*]	5.22
$\Gamma_{15}^V - X_1^C (eV)$	2.18 [*]	2.19
$\Gamma_{15}^V - L_1^C (eV)$	3.40 [*]	3.34

Table 2: Key energies at selected symmetry points in the Brillouin Zone [22]. Values denoted by asterisks are used in the present work.

	$\frac{dE_{nk}}{dp} (10^{-2} \frac{eV}{GPa})$		$\frac{d^2E_{nk}}{dp^2} (10^{-7} \frac{eV}{GPa^2})$	
Γ_1^C	8.54 ^a	5.50 ^b	-4.54 ^a	-2.97 ^b
X_1^C	-0.37 ^a	-0.34 ^b	0.39 ^a	0.0106 ^b
L_1^C	3.98 ^a	3.95 ^b	-4.66 ^a	-1.58 ^b

Table 3: Linear and quadratic pressure coefficients of important band gaps for BP. In our study, we take the pressure coefficients given by [9]. ^a : Ref. [9], ^b : Ref. [12]

Pressure (GPa)	Lattice parameter a (10 ⁻¹ nm)	E _{ΓΓ} (eV)	E _{ΓX} (eV)	E _{ΓL} (eV)
0	4.53000	5.2500	2.1800	3.4000
10	4.45130	6.0586	2.1469	3.7514
20	4.38665	6.7764	2.1216	4.0096
30	4.33194	7.4034	2.1041	4.1746
40	4.28457	7.9396	2.0944	4.2464
50	4.24290	8.3850	2.0925	4.3050
60	4.20568	8.7396	2.0984	4.3704
70	4.17212	9.0034	2.1121	4.4426
80	4.14158	9.1764	2.1336	4.5016
90	4.11358	9.2586	2.1629	4.5574
100	4.08774	9.2500	2.2000	4.6150
120	4.04141	8.9604	2.2976	4.6726
140	4.00080	8.3076	2.4264	4.7301

Table 4: The calculated fundamental energy gaps of boron phosphide versus hydrostatic pressure.

In an attempt to give a qualitative idea of the expected pressure dependence of the pseudopotential form factors of boron phosphide, a least squares fit exhibits a sublinearity, yielding linear b and quadratic c coefficients:

$$V_p(G^2) - V_0(G^2) = bp + cp^2 \quad (21)$$

where $V_p(G^2)$ is the fitted form factor at pressure p.

The variations of the pseudopotential form factors $V_p(G^2)$ with pressures are illustrated in the table 5. We give the lattice parameters at each pressure and also the best fit of the dependence of form factors on pressure. The antisymmetric form factors $V_a(3)$ and $V_a(4)$ remains unchanged under different pressures. We give also the best fit of the dependence of form factors on pressure:

$$\begin{aligned} V_s(3) &= -0.379 + 2.4 \times 10^{-3}p - 1.72 \times 10^{-5}p^2 \\ V_s(8) &= 0.0803 - 1.93 \times 10^{-3}p + 1.165 \times 10^{-5}p^2 \\ V_s(11) &= 0.0989 + 4.55 \times 10^{-3}p - 2.585 \times 10^{-5}p^2 \\ V_a(11) &= 0.04744 + 0.807 \times 10^{-3}p - 0.571 \times 10^{-5}p^2 \end{aligned}$$

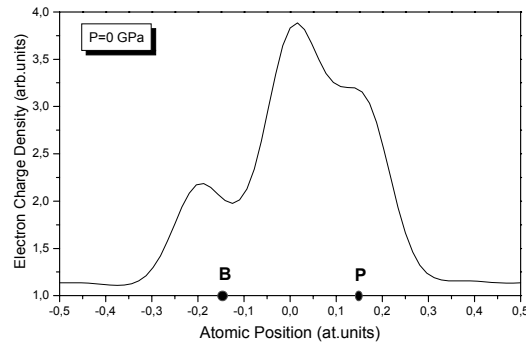
To analyze the evolution of the bonding properties, we have computed the pseudo-valence band charge densities at the high symmetry point Γ along the $\langle 111 \rangle$ direction (the axis bond), for different pressures.

P (GPa)	Lattice Parameter a (at.unit)	$V_s(3)$	$V_s(8)$	$V_s(11)$	$V_a(3)$	$V_a(4)$	$V_a(11)$	Rms (eV)
0	8.560576	-0.385497	0.0870	0.101625	0.010	0.023	0.051500	0.00051
20	8.289693	-0.330486	0.041130	0.180770	0.010	0.023	0.060574	0.00057
40	8.096786	-0.307840	0.013742	0.237385	0.010	0.023	0.060574	0.00063
60	7.947687	-0.297674	0.006871	0.279549	0.010	0.023	0.079312	0.00089
80	7.826567	-0.297512	0.006871	0.299740	0.010	0.023	0.080650	0.00039
100	7.724821	-0.313254	0.006871	0.296123	0.010	0.023	0.079530	0.00045
120	7.637258	-0.342269	0.009954	0.266681	0.010	0.023	0.049525	0.00052
140	7.560512	-0.374427	0.036001	0.231060	0.010	0.023	0.049525	0.00046

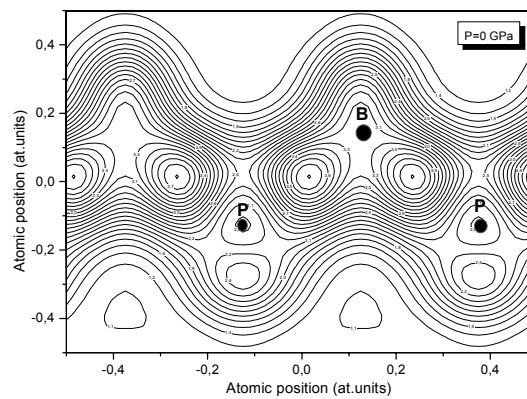
Table 5: The adjusted pseudo potential form factors of BP are given in Rydberg.

Figure 1-a and figure 1-b display the total valence charge densities at the normal pressure along the $\langle 111 \rangle$ axis and in the $(1\bar{1}0)$ plane, respectively. We notice that the charge density is optimal between B and P atoms, which indicate a strong covalent character of this compound. There is also a consistent charge around the P core. This behaviour results from the contribution of the first band and the upper three valence bands as was seen in figure 2. We find that the lowest band is mainly contributed by the s state of the P atom.

However, the upper three valence bands have comparable contribution from the p states of both B and P atoms. This is consistent with the fact that their configurations of outer electrons in the ground atomic states are: $2s^22p$ for the B atom and $3s^23p^3$ for the P atom.



(a)



(b)

Fig. 1: The total valence charge densities of boron phosphide at normal pressure: (a): along the $\langle 111 \rangle$ direction. (b): in the $(1 \bar{1} 0)$ plane.

Under pressure (figure 3), we notice that the total charge densities for the BP show a qualitative as well as a quantitative changes. Hence, from $p=0$ to 140 GPa, the maximum of charge is more pronounced for 60 GPa than that of 0 GPa and 140 GPa. However, around the P anion the situation is quite different because the maximum of charge is more important at $p=0$ GPa than at $p=60$ and 140 GPa. We can also notice that there is a charge rearrangement since there is a charge transfer to the interstitial sites. For the more explanation of this behaviour, we have displayed, in figure 4 and figure 5, the contribution of the four valence bands to the total distribution at 60 GPa and 140 GPa, respectively.

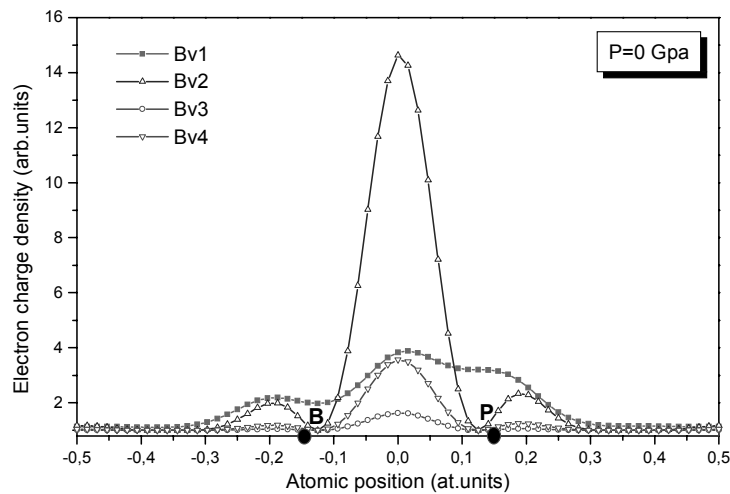


Fig. 2: Electron charge contribution of each valence band to the total valence charge density at normal pressure $p=0$ GPa: (Bv₁: first valence band; Bv₂: second valence band; Bv₃: third valence band and Bv₄: fourth valence band).

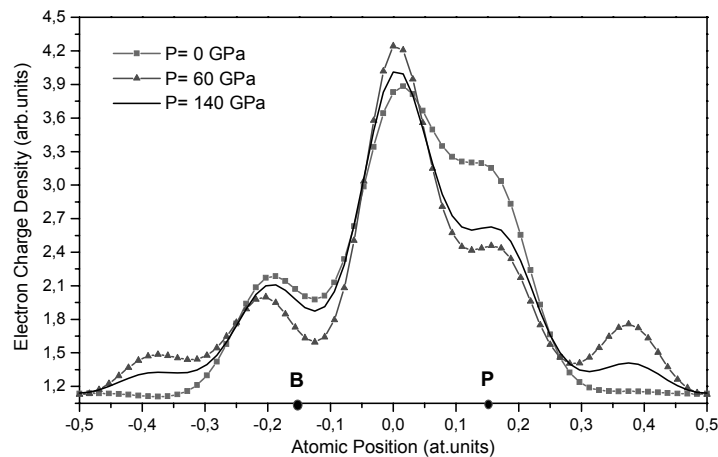


Fig. 3: The total valence charge densities of BP along the $\langle 111 \rangle$ direction at $p=0$, 60 and 140 GPa.

When the pressure increases (figure 4) from 0 GPa to 60 GPa, we notice that the covalent character is due to the contribution of the second and the fourth valence bands. The lowest valence band shows an s-like character.

Going from 60 GPa to 140 GPa (figure 5), we notice that the covalent character is a consequence of the contribution of the second and the third valence bands corresponding to the p-like character. The first valence band show the similar kind compared to that of the figure 4. As a consequence, we can state that under pressure the boron phosphide is found theoretically to behave anomalously [10]. The chemical explanation of this phenomenon is simple. According to the Phillips and Van Vechten scale of ionicities, BP is one of the least ionic compounds of the III-V family ($f_i=0.006$). The very attractive B potential competes with the P potential for the valence charge, creating a situation of small heteropolarity and consequently small ionicity.

We start to discuss the results of the thermalized positron charge density at Γ_1 along the $\langle 111 \rangle$ direction, in order to analyze the behaviour of positron in this compound.

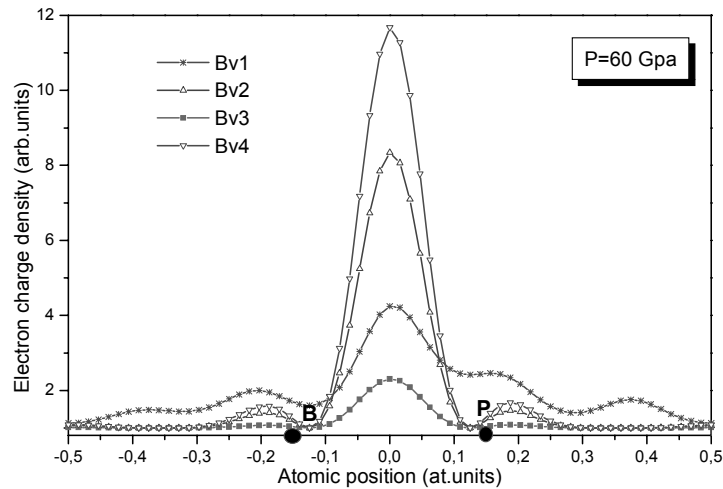


Fig. 4: Electron charge contribution of each valence band to the total valence charge density at $p= 60$ GPa: (Bv₁: first valence band; Bv₂: second valence band; Bv₃: third valence band and Bv₄: fourth valence band).

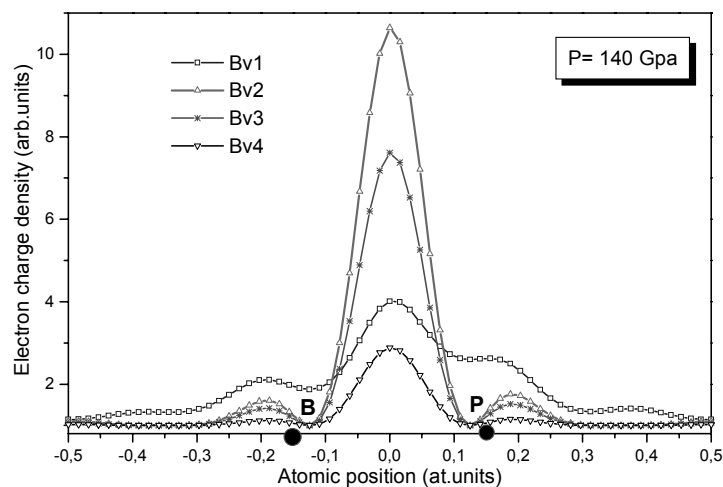


Fig. 5: Electron charge contribution of each valence band to the total valence charge density at $p= 140$ GPa: (Bv₁: first valence band; Bv₂: second valence band; Bv₃: third valence band and Bv₄: fourth valence band).

At the normal pressure, we have plotted the positron charge distribution along the $\langle 111 \rangle$ direction and in the $(1\bar{1}0)$ plane (fig 6-a, fig 6-b), there is a clear assymetrical distribution of the positron relative to the bond center. In this region, the positron charge is less significant. Hence,

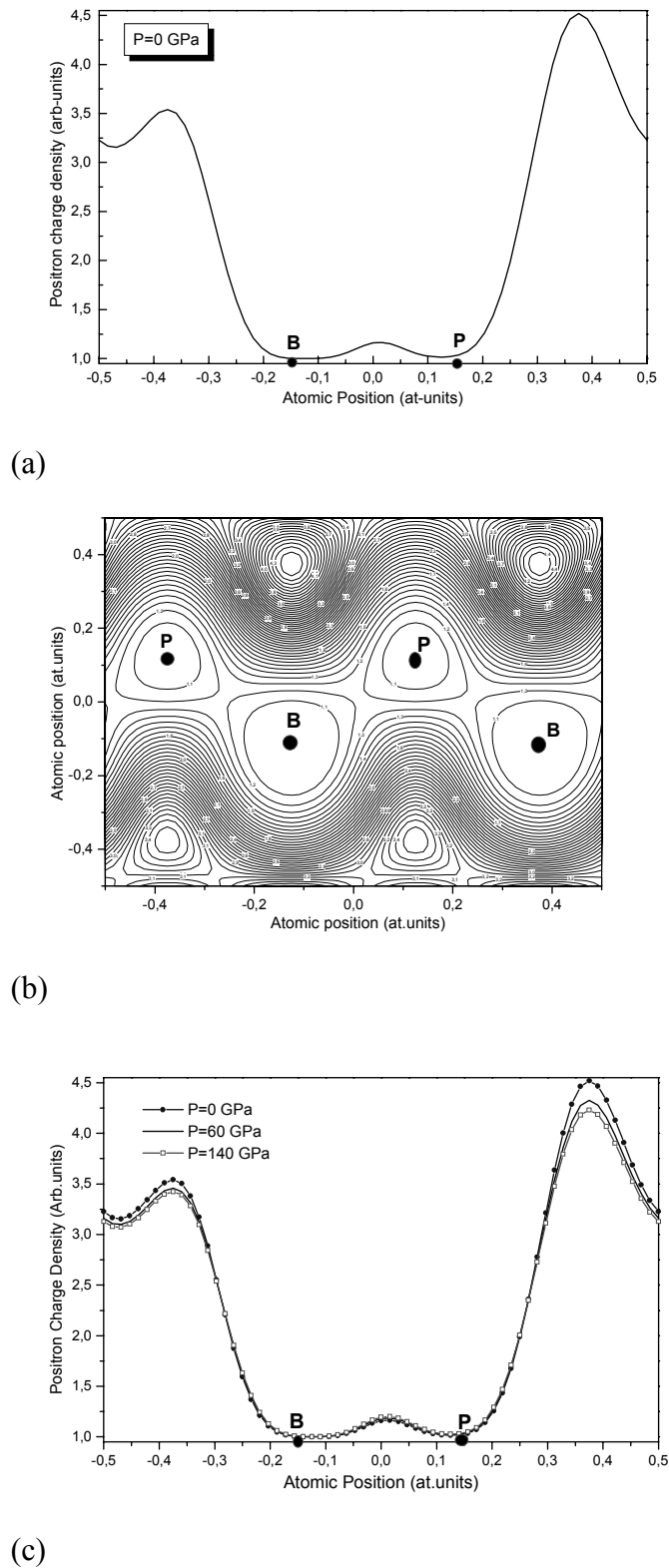


Fig. 6: The positron charge densities of BP at Γ_1 point: (a): along the $\langle 111 \rangle$ direction, at normal pressure. (b): in the $(1 \bar{1} 0)$ plane, at normal pressure. (c): along the $\langle 111 \rangle$ direction, at $p=0, 60$ and 140 GPa.

the preferential sites for the positron are the cation and the anion interstitial regions, where the distributions are more significant. This is consistent with the fact that the positron is repelled by the positively charged cores. This behaviour is similar to that found for the III-V compounds. However, there is a qualitative difference if we take into account the characteristic of each atom which contributes to the bonding. Hence, the positron tends to be pushed out of the cell containing the larger valence and larger ion core. This is the case of phosphorous atom which has the larger valence than boron ones. This is the reason why the positron is attracted to the cell with larger electron density.

Figure 6-c gives a comparison between the behaviour of the positron for different pressures (60 and 140 GPa). It was seen that when the pressure increases, the distribution of charge relative to the interstitial sites decreases but increases less significantly in the internuclear spacing. This is consistent with the fact that the applied pressure reduces the interstitial volume preferred by a positron and hence leads to greater positron penetration into the region of the ion cores.

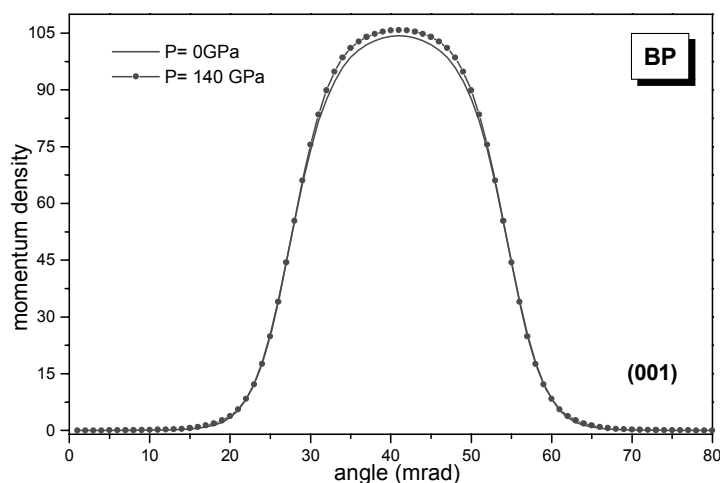


Fig. 7: The integrated electron-positron momentum densities of boron phosphide along the (001) direction at $P = 0$ and 140 GPa.

To combine the effect of the electron and the positron wave functions, we have plotted, in figure 7 and figure 8, the integrated electron-positron momentum densities in BP along the (001) and (110) directions, respectively. It was seen that there are a clear continuous contributions, i.e. there are no breaks in the distributions and thus, all the bands are full. One can also notice that in the regime of large momentum, the profile is flat in the (001) direction but is sharply peaked along the (110) direction. The flatness in the peaks along the (001) direction and the sharp peaks along the (110) direction could be understood in terms of the contribution from σ and π bonding orbitals to the ideal sp^3 hybrid bands.

It is known that the interaction between the second neighbour σ bands is equivalent to an π anti bonding interaction between neighbouring atoms. As a consequence, there is a strong $(2p, 3p)\sigma$ bond along the (110) direction and an admixture of $(2p, 3p)\sigma$ and $(2p, 3p)\pi$ bonds along the (001) direction in the case of the boron phosphide. When the pressure is applied, the momentum

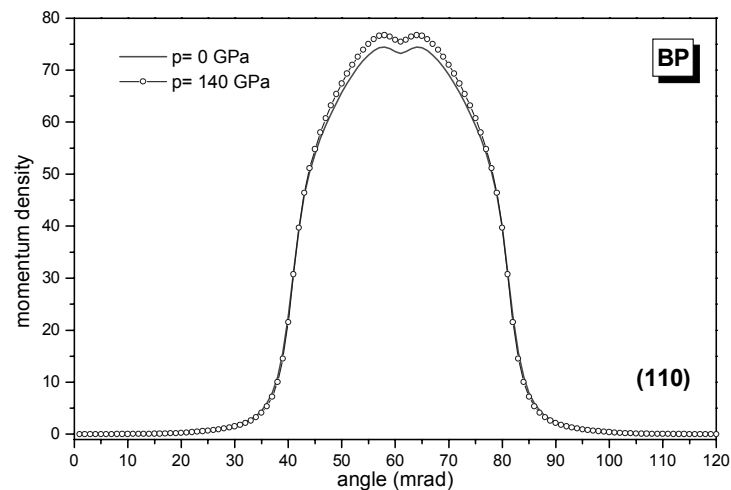


Fig. 8: The integrated electron-positron momentum density of boron phosphide along the (110) direction at $p = 0$ and 140 GPa.

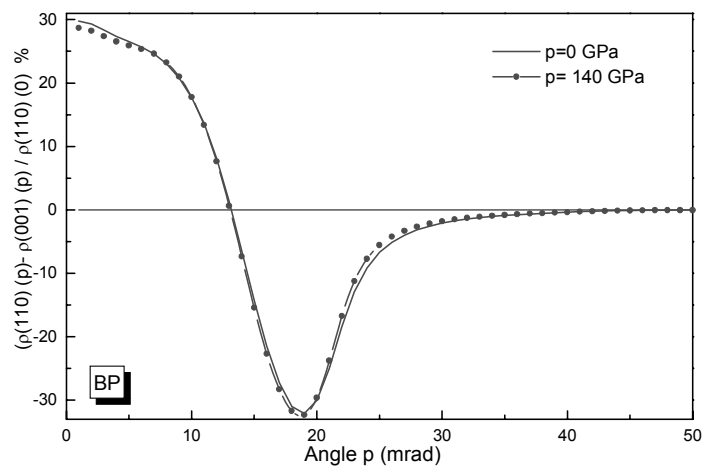


Fig. 9: The relative positron anisotropies of BP at $p = 0$ and 140 GPa.

density tends to be much flatter in both directions, this could be ascribed to the fact that the extra π^* interaction is stronger. This is also a consequence of the distortion of the electron and the positron wave functions caused by the reduction of the lattice volume. This discrepancy in the two profiles could be considered as anisotropy of their wave functions. The percentage anisotropies of the momentum densities are displayed in figure 9. The percentage anisotropies at 140 GPa is seen to be above that at 0 GPa especially in the regime of large momentum. On one hand, we can state that both the electron and the positron wave functions are anisotropic and, on other hand, the effect of the applied pressure is to reduce the anisotropy in the lattice.

4. Conclusion

We have successfully applied the empirical pseudopotential method (EPM) and the independent particle approximation (IPM) to calculate the electronic and the positronic properties of BP under pressure. The obtained results show that the band structure is distortion by the pressure variations due to the fact that the principal band gaps change with pressure variations. The results of the electron and the positron charge distributions confirm that the bonding properties also change with pressure. These changes have immediate consequences on the electron-positron momentum density, especially in the regime of large momentum. Finally, the percentage anisotropy is seen to be significantly changed when the pressure is applied.

References

- [1] J. T. Glass, R. Messier, N. Fujimori (Ed) *Diamond, Silicon carbide and related wide band gap semiconductors*, MRS Symp. Proc. No. 162, Pittsburgh, PA: Materials Research Society (1990)
- [2] Y. Kumashiro, *J. Mater. Res.* **5** (1990) 2933
- [3] J. C. Phillips, *Bonds and Bands in semiconductors*, Academic press, New York (1973)
- [4] P. Rodriguez-Hernandez, M. Gonzalez-Diaz, A. Muñoz, *Phys. Rev. B* **51** (1995) 14705
- [5] A. Lichanot, M. Causà, *J. Phys: Cond. Matter* **9** (1997) 3139
- [6] W. R. L. Lambrecht, B. Segall, *Phys. Rev. B* **43** (1991) 7070
- [7] R. Orlando, R. Dovesi, C. Roetti, V. R. Saunders, *J. Phys: Cond. Matter.* **2** (1990) 7769
- [8] H. Xia, Q. Xia, A. L. Ruoff, *J. Appl. Phys.* **74** (1993) 1660
- [9] B. Bouhafs, H Aourag and M. Certier, *J. Phys: Cond. Matter* **12** (2000) 5655
- [10] R. M. Wentzcovitch, P. K. Lam, M. L. Cohen, *Phys. Rev. B* **36** (1987) 6058
- [11] R. M. Wentzcovitch, K. J. Chang, M. L. Cohen, *Phys. Rev. B* **34** (1986) 1071
- [12] B. H. Cheong, K. J. Chang, M. L. Cohen, *Phys. Rev. B* **44** (1991) 1053
- [13] R. R. Hasiguti, K. Fujiwara (Ed.), *Proc.5th Inter. Conf. Positron Annihilation*, Academic Press, Sendai (1979)
- [14] M. J. Puska, *J. Phys: Cond. Matter.* **3** (1991) 3455
- [15] A. Belaidi, R. N. West, *Phys. Stat. Sol (a)* **102** (1987) 107
- [16] A. Belaidi, R. N. West, *J. Phys. F* **18** (1988) 1001
- [17] S. L. Richardson, M. L. Cohen, *Phys. Rev. B* **35** (1987) 1388
- [18] D. Stroud, H. Ehrenreich, *Phys. Rev.* **171** (1968) 399
- [19] H. Nara, M. J. Schlesinger, *Phys. C. Solid State Physics* **5** (1972) 606
- [20] J. A. Sanjurjo, E. Lôpez-Cruz, P. Vogl, M. Cardona, *Phys. Rev. B* **28** (1983) 4579
- [21] R. C. Weast, M. J. Astle, W. H. Beyer, *Handbook of chemistry and physics*, 67th edition West Palm Beach, FL: Chemical Rubber Company Press (1987)
- [22] N. Badi, H. Abid, M. Driz, N. Amrane, B. Soudini, B. Khelifa and H. Aourag, *Phys. Stat. Sol (b)* **186** (1994) 379